

JWST Spectroscopic View of a Rapidly Growing Dust-obscured Quasar at $z \sim 4$: Effect of Dust Extinction Correction on Black Hole Mass and Eddington Ratio Estimation

DOHYEONG KIM¹ AND MYUNGSHIN IM^{2,3}

¹*Department of Earth Sciences, Pusan National University, Busan 46241, Republic of Korea*

²*Astronomy Program, Dept. of Physics & Astronomy, Seoul National University, Seoul 08826, Republic of Korea*

³*SNU Astronomy Research Center (SNU ARC), Astronomy Program, Dept. of Physics & Astronomy, Seoul National University, Seoul 08826, Republic of Korea*

ABSTRACT

In the merger-driven galaxy evolution scenario, the central supermassive black holes (SMBHs) in dust obscured galaxies grow rapidly. Interestingly, a recent work (Suh et al. 2024) on a dust-obscured galaxy, LID-568 at $z = 3.965$, has shown that its SMBH is growing extremely fast at about 40 times of the Eddington-limited accretion rate (i.e., super-Eddington accretion). However, the heavy dust extinction of the host galaxy could affect the result if not corrected properly. Here, we analyze James Webb Space Telescope (JWST) NIRSpec/IFU and MIRI spectra of LID-568. By measuring its bolometric luminosity (L_{bol}) and BH mass (M_{BH}) using an extinction-free estimator based on mid-infrared spectra, we obtain $L_{\text{bol}} = 10^{46.83 \pm 0.07} \text{ erg s}^{-1}$ and $M_{\text{BH}} = 10^{8.43 \pm 0.15} M_{\odot}$. The measured Eddington ratio (λ_{Edd}) is 1.97 ± 0.88 , consistent with the accretion rate at the Eddington limit; in other words, not in super-Eddington in a significant manner. This result underscores challenges and the importance of carefully considering dust extinction when analyzing the BH growth in dust-obscured quasars.

Keywords: Galaxy evolution (594) — Early universe (435) — Supermassive black holes (1663) — Quasars (1319) — James Webb Space Telescope (2291) — Infrared astronomy (786)

1. INTRODUCTION

SMBHs have been found at the centers of spheroidal galaxies, with their masses tightly correlating with several properties of their host galaxies (e.g., bulge mass, stellar velocity dispersion, stellar mass, etc.; Ferrarese & Merritt 2000; Gebhardt et al. 2000; Kormendy & Ho 2013). It is uncertain how SMBHs were born and grew, but several simulation studies (e.g., Hopkins et al. 2006, 2008) suggest that dust-obscured quasars are a key to understand the SMBH growth process. According to such studies, dust-obscured quasars represent the intermediate stage between the merger-driven star-forming galaxies and unobscured quasars. In this merger-driven galaxy evolution scenario, the SMBHs in dust-obscured quasars are expected to be growing very rapidly, sometimes in well-above the Eddington-limited accretion rate (super-Eddington ac-

cretion; e.g., Hopkins et al. 2008). Several observational studies (e.g., Urrutia et al. 2012; Kim et al. 2015, 2024b) find that dust-obscured quasars are accreting matters at near the Eddington limit, supporting this scenario. Moreover, further support for the merger-driven galaxy evolution scenario comes from several pieces of observational evidence. For example, dust-obscured quasars exhibit (i) significant merging signatures in their host galaxies (Urrutia et al. 2008; Glikman et al. 2015); (ii) dusty red colors (Kim & Im 2018); (iii) merging SMBH candidates (Kim et al. 2020); and (iv) enhanced star-forming activities (Georgakakis et al. 2009). A few studies have found high redshift dust-obscured quasars with the Eddington ratios of a few (Tsai et al. 2018; Finnerty et al. 2020; Jun et al. 2020; Kim et al. 2024a). However, large scatters in scaling relations and uncertainties in dust-extinction correction make it difficult to conclusively claim that such quasars are undergoing super-Eddington accretion. Much stronger evidence for super-Eddington accretion is therefore required.

Recently, [Suh et al. \(2024\)](#) reported the discovery of a long-sought dust-obscured quasar at $z \simeq 4$ that is undergoing a strong super-Eddington accretion. They analyzed X-ray, infrared (IR), and JWST spectroscopic data to find the Eddington ratio of about 40 for this quasar, LID-568, which is well above the Eddington ratio of one for Eddington-limited accretion.

One significant difficulty in such a study is the heavy extinction which complicates the measurement of the black hole mass, bolometric luminosity, and Eddington ratio. [Suh et al. \(2024\)](#) found that the bolometric luminosity from the 5100 Å continuum luminosity is about a factor of 10 lower than the X-ray based value. They also found an Eddington ratio to be 4.4 when using an internally consistent method of deriving the Eddington ratio from H α line.

In this study, we measure the L_{bol} and M_{BH} values of LID-568 using estimators designed to minimize the effects of dust extinction by using mid-infrared (MIR) continuum luminosity and the velocity width of the H α line ([Kim et al. 2023](#)). Subsequently, we compare the newly-derived λ_{Edd} to other quasars at similar redshifts. Throughout, we use a standard Λ CDM model of $H_0 = 70 \text{ km s}^{-1} \text{ Mpc}^{-1}$, $\Omega_m = 0.3$, and $\Omega_\Lambda = 0.7$, which has been supported by several observational studies (e.g. [Im et al. 1997](#); [Planck Collaboration et al. 2016](#)).

2. LID-568

LID-568 is an dust-obscured quasar, originally identified as a near-infrared (NIR) dropout object and later as an X-ray source in the *Chandra*-COSMOS Legacy Survey ([Civano et al. 2016](#); [Marchesi et al. 2016](#)). Follow-up JWST NIRSpec and MIRI observations revealed that its redshift is 3.965, and it has a very red continuum ([Suh et al. 2024](#)). Furthermore, strong and broad hydrogen lines were detected, as shown in Figure 1, providing a supporting evidence that LID-568 is a dust-obscured quasar. The L_{bol} from X-ray and M_{BH} from the JWST rest-frame optical spectrum provided the λ_{Edd} of ~ 40 ([Suh et al. 2024](#)).

3. DATA ANALYSIS

3.1. Spectral energy distribution fitting

[Kim et al. \(2023\)](#) established new L_{bol} and M_{BH} estimators for dust-obscured quasars, which were derived based on the continuum luminosities at 3.4 μm and 4.6 μm (hereafter, $L_{3.4}$ and $L_{4.6}$, respectively) in the rest-frame. Here, we perform an SED fitting using the JWST NIRSpec and MIRI spectra for obtaining the $L_{3.4}$. The JWST spectra [$f(\lambda)$] are fit with a reddened quasar spectrum [$Q(\lambda)$], as $f(\lambda) = CQ(\lambda)$, where C is the normalization constant. Here, the $Q(\lambda)$ is

reddened from an unobscured quasar spectrum [$Q_0(\lambda)$; [Assef et al. 2010](#)] using a reddening law based on Small Magellanic Cloud bar dust extinction curve with $R_V = 2.74$ ([Gordon et al. 2003](#)). Note that even if the Galactic dust extinction curve with $R_V = 3.1$ ([Fitzpatrick 1999](#)) is adopted instead, the derived $L_{3.4}$ shows no significant ($< 5\%$) difference.

Meanwhile, [Kim et al. \(2023\)](#) used several types of galaxy spectra in their SED fitting, but for LID-568, we adopt the result where only the $Q(\lambda)$ component is employed. We attempted the SED fitting including the galaxy spectra as done by [Kim et al. \(2023\)](#), but the galaxy contributions to the SED are found to be negligible. Moreover, we adopt the quasar spectrum of [Assef et al. \(2010\)](#) for this work, as it yields the best reduced chi-square fit compared to using other quasar spectra from [Richards et al. \(2006\)](#) and [Krawczyk et al. \(2013\)](#). However, regardless of which quasar spectrum is used for the fitting, the measured $L_{3.4}$ does not vary significantly ([Kim et al. 2023](#)), and the discrepancy is added as an uncertainty in quadrature to its original uncertainties obtained from the SED fit.

For the SED fitting, we use the MPFIT procedure ([Markwardt 2009](#)), and Figure 1 shows the best-fit model. Through the SED fitting, we obtain a color excess, $E(B-V)_{\text{SED}}$, to be 2.29 ± 0.29 , and the extinction-corrected $L_{3.4}$ is $10^{46.11 \pm 0.06} \text{ erg s}^{-1}$.

3.2. Emission line fitting

In this subsection, we describe how H α , P β , and P α lines are fit with the JWST NIRSpec and MIRI spectra. First, we fit the continua around these lines with a single power law. After that, the emission lines are fit with a single or double Gaussian function, and Figure 2 shows the emission lines and their best-fit models.

[Kim et al. \(2010\)](#) showed that the measured fluxes and FWHMs fit with the single, double, and multiple Gaussian functions can be biased, and provided the correction factors. The correction factors are $\text{flux}_{\text{multi}}/\text{flux}_{\text{single}} = 1.06$, $\text{flux}_{\text{multi}}/\text{flux}_{\text{double}} = 1.05$, $\text{FWHM}_{\text{multi}}/\text{FWHM}_{\text{single}} = 0.91$, and $\text{FWHM}_{\text{multi}}/\text{FWHM}_{\text{double}} = 0.85$. These factors represent the average ratios, with individual quasars exhibiting values ranging from ~ 0.75 to ~ 1.2 ([Kim et al. 2010](#)). In this study, the measured line properties are corrected to those measured using the multi Gaussian function fitting.

We fit the H α line with a double Gaussian function, whereas the P β and P α lines are fitted with a single Gaussian function due to the poor S/N and spectral resolution of the spectrum, as shown in Figure 2. The measured FWHM and flux of the H α line are

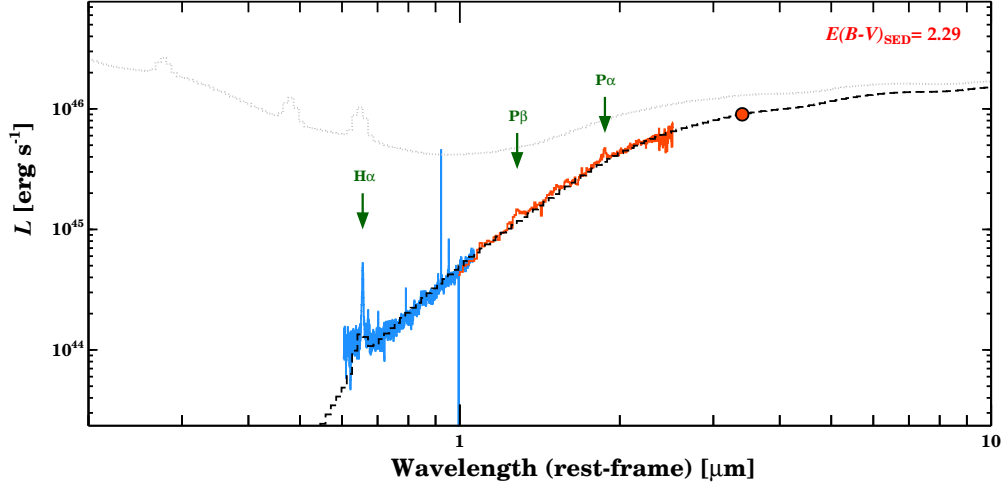


Figure 1. JWST spectra and best-fit SED model. Blue and red lines represent NIRSpec and MIRI spectra, respectively. Black dashed line and gray dotted line indicate the best-fit model and the extinction-corrected best-fit model, respectively. Red circle represents $L_{3.4}$ of the best-fit model. $H\alpha$, $P\beta$, and $P\alpha$ lines are marked with green arrows.

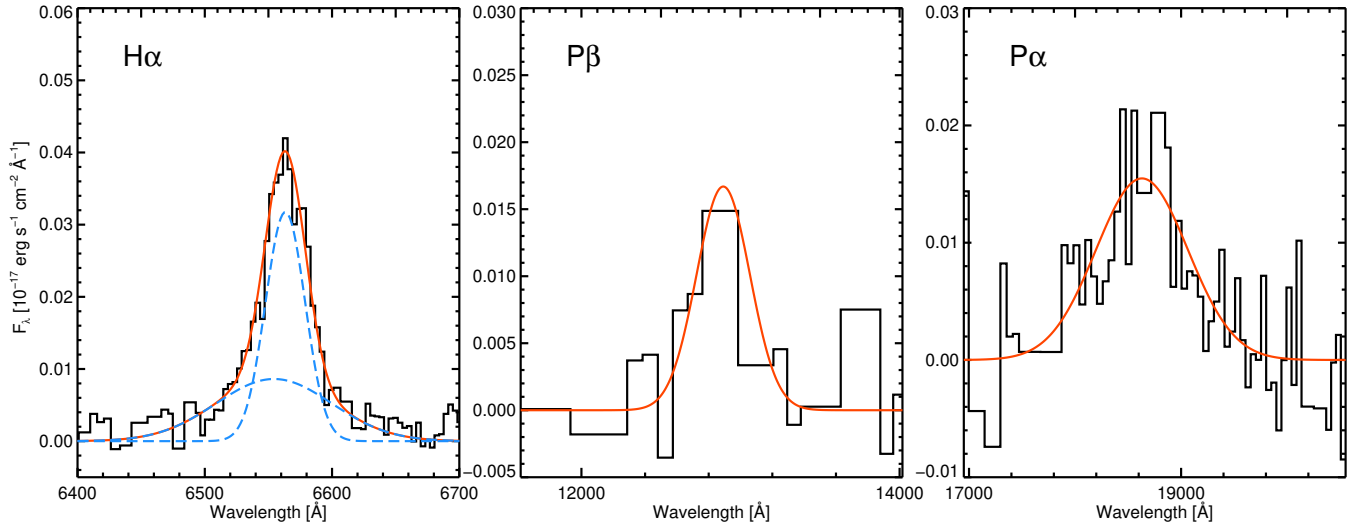


Figure 2. Fitting results for the $H\alpha$, $P\beta$, and $P\alpha$ lines. The black and red solid lines represent the continuum-subtracted spectra and the best-fit models, respectively. The $H\alpha$ line is fit with a double-Gaussian function, and each component is presented as the blue dashed line.

$1610 \pm 80 \text{ km s}^{-1}$ and $(2.33 \pm 0.20) \times 10^{-17} \text{ erg s}^{-1} \text{ cm}^{-2}$, respectively, and the measured FWHM value is corrected for the instrumental resolution. Note that we also fit the $H\alpha$ line with a single Gaussian function, yielding $\frac{\text{FWHM}_{H\alpha}(\text{double})}{\text{FWHM}_{H\alpha}(\text{single})}$ and $\frac{\text{flux}_{H\alpha}(\text{double})}{\text{flux}_{H\alpha}(\text{single})}$ are ~ 0.9 and ~ 1.1 , respectively. These ratios are consistent with the FWHM and flux ratios of the quasars used to derive the correction factors.

For the $P\beta$ and $P\alpha$ lines, we only measure their fluxes due to the poor S/N and spectral resolution of the spectrum. The measured $P\beta$ and $P\alpha$ line fluxes are $(7.44 \pm 0.64) \times 10^{-17}$ and

$(17.8 \pm 0.9) \times 10^{-17} \text{ erg s}^{-1} \text{ cm}^{-2}$, respectively. Using these fluxes, we measure the color excess, $E(B-V)_{\text{line}}$, to be 2.69 ± 0.11 based on the method of Kim et al. (2018), which is a bit larger than the $E(B-V)_{\text{SED}}$ but can be taken as a consistent value considering simplified assumptions for the fit. Note that, in this study, the extinction correction is performed using the $E(B-V)_{\text{SED}}$ instead of the $E(B-V)_{\text{line}}$ due to the poor quality of the Paschen line spectra.

4. RESULTS

4.1. Bolometric luminosity and BH mass

To measure the bolometric luminosity, we use the $L_{3.4}$ -based L_{bol} estimator (Kim et al. 2023), which is

$$\log\left(\frac{L_{\text{bol}}}{10^{44} \text{ erg s}^{-1}}\right) = (0.718 \pm 0.011) + \log\left(\frac{L_{3.4}}{10^{44} \text{ erg s}^{-1}}\right). \quad (1)$$

Using the extinction-corrected $L_{3.4}$, the measured L_{bol} is found to be $10^{46.83 \pm 0.07} \text{ erg s}^{-1}$. Additionally, we measure the L_{bol} value using the extinction-corrected $L_{\text{H}\alpha}$. To obtain the $L_{\text{H}\alpha}$ -based L_{bol} , we use several relations between the $L_{\text{H}\alpha}$, continuum luminosity at 5100 Å (L5100), and L_{bol} . We bootstrap the relation between $L_{\text{H}\alpha}$ and L5100 (Greene & Ho 2005), and between L5100 and L_{bol} (Richards et al. 2006), as done in Suh et al. (2024). Using the combined relation, the $L_{\text{H}\alpha}$ -based L_{bol} is found to be $10^{46.46 \pm 0.04} \text{ erg s}^{-1}$, which is slightly smaller than the L_{bol} derived from $L_{3.4}$, considering the scatter of 0.13 dex in the relation (Kim et al. 2023). Note that, in this study, the L_{bol} from $L_{3.4}$ is used instead of the $L_{\text{H}\alpha}$ -based L_{bol} . This is because, even after applying dust-extinction correction, the $L_{\text{H}\alpha}$ -based L_{bol} is sensitive to uncertainties in the $E(B-V)$ measurement, whereas the $L_{3.4}$ -based L_{bol} is less affected by such uncertainties.

Furthermore, we also measure L_{bol} based on $L_{\text{P}\beta}$ and $L_{\text{P}\alpha}$ using Paschen-line-based L_{bol} estimators (Kim et al. 2022). We use the extinction-corrected Paschen line luminosities, and the $L_{\text{P}\beta}$ - and $L_{\text{P}\alpha}$ -based L_{bol} values are found to be $\sim 10^{46.7} \text{ erg s}^{-1}$, which are consistent with our $L_{3.4}$ - and $L_{\text{H}\alpha}$ -based L_{bol} values.

Note that Suh et al. (2024) also measured the L_{bol} using X-ray data, an SED fitting, and $L_{\text{H}\alpha}$. The L_{bol} values from the X-ray and SED fitting were $\sim 10^{46.6} \text{ erg s}^{-1}$, which is consistent with our measurements. However, the L_{bol} from $L_{\text{H}\alpha}$ was only $10^{45.6} \text{ erg s}^{-1}$, which is 10 times smaller than our measurement, demonstrating the importance of dust-extinction correction when deriving physical quantities of quasars from the rest-frame optical spectrum.

We measure M_{BH} based on $L_{3.4}$ and $\text{FWHM}_{\text{H}\alpha}$ (Kim et al. 2023), which is

$$\log\left(\frac{M_{\text{BH}}}{M_{\odot}}\right) = (6.952 \pm 0.059) + 0.5 \log\left(\frac{L_{3.4}}{10^{44} \text{ erg s}^{-1}}\right) + (2.06 \pm 0.06) \log\left(\frac{\text{FWHM}_{\text{H}\alpha}}{10^3 \text{ km s}^{-1}}\right). \quad (2)$$

The measured M_{BH} is $10^{8.43 \pm 0.15} M_{\odot}$, and our measurement is ~ 40 times higher than the M_{BH} , $\sim 10^{6.86} M_{\odot}$, measured in Suh et al. (2024).

Note that Suh et al. (2024) measured the M_{BH} using the $\text{H}\alpha$ line-based estimator (Greene & Ho 2005). We also measure the M_{BH} using the $\text{H}\alpha$ line-based estimator

with the extinction-corrected $L_{\text{H}\alpha}$ and the $\text{FWHM}_{\text{H}\alpha}$. The obtained M_{BH} is $10^{8.04 \pm 0.19} M_{\odot}$, which is in line with the $L_{3.4}$ -based M_{BH} . Suh et al. (2024) and we obtained flux and FWHM values of the $\text{H}\alpha$ line that are very similar to each other. The discrepancy in M_{BH} is mainly caused by differences in extinction correction.

Additionally, we also measure M_{BH} based on $L_{\text{P}\beta}$ and $L_{\text{P}\alpha}$ using the Paschen-line-based estimators (Kim et al. 2022). To obtain the Paschen-line-based M_{BH} , Paschen line luminosity and FWHM values are necessary, and the $\text{FWHM}_{\text{P}\beta}$ and $\text{FWHM}_{\text{P}\alpha}$ values are converted from the $\text{FWHM}_{\text{H}\alpha}$ (Kim et al. 2010). With the extinction-corrected $L_{\text{P}\beta}$ and $L_{\text{P}\alpha}$, we measure the $\text{P}\beta$ - and $\text{P}\alpha$ -based M_{BH} values, which are $\sim 10^{8.2} M_{\odot}$. These measurements agree with the $L_{3.4}$ - and $L_{\text{H}\alpha}$ -based M_{BH} values, and significantly higher than that of Suh et al. (2024).

4.2. Eddington ratio

We measure λ_{Edd} using the newly measured L_{bol} and M_{BH} values. If we use the $L_{3.4}$ -based M_{BH} , λ_{Edd} is found to be 1.97 ± 0.88 , suggesting that LID-568 exhibits super-Eddington BH accretion activity only at a modest level. However, our measurement is significantly smaller than the λ_{Edd} of 41.5 measured in Suh et al. (2024). This discrepancy is mainly due to the differences in the M_{BH} measurements. Note that, if the $L_{\text{H}\alpha}$ -based M_{BH} is adopted, λ_{Edd} increases to 4.83 ± 2.86 , similar to the $\text{H}\alpha$ -based λ_{Edd} value in Suh et al. (2024).

In Figure 3a, we compare the L_{bol} versus M_{BH} of LID-568 with quasars at $z \sim 4-7$. The measured λ_{Edd} of LID-568 is comparable to the highest λ_{Edd} values of quasars at $z \sim 4-7$ (Tsai et al. 2018; Finnerty et al. 2020; Harikane et al. 2023; Matthee et al. 2024; Farina et al. 2022; Maiolino et al. 2023; Greene et al. 2024). Note that these comparisons cover various types of quasars, including dust-obscured quasars. Overall, our result indicates that LID-568 harbors a rapidly growing SMBH at around the Eddington limit.

Finally, we remark that recent observational studies (e.g., Du et al. 2016; Du & Wang 2019; GRAVITY Collaboration et al. 2024) have shown that quasars with high luminosities and high λ_{Edd} values could have smaller broad line region (BLR) sizes by factors of a few, compared to those expected from well-known $R_{\text{BLR}}-L$ relationships. If this is true, high- λ_{Edd} quasars tend to have overestimated M_{BH} values, implying that LID-568's M_{BH} and λ_{Edd} may deviate from the measured quantities, tending toward a lower M_{BH} and higher λ_{Edd} . However, in such a case, all other points near $\lambda_{\text{Edd}} \sim 1$ would move leftward (higher λ_{Edd} values by a factor of a few) in Figure 3.

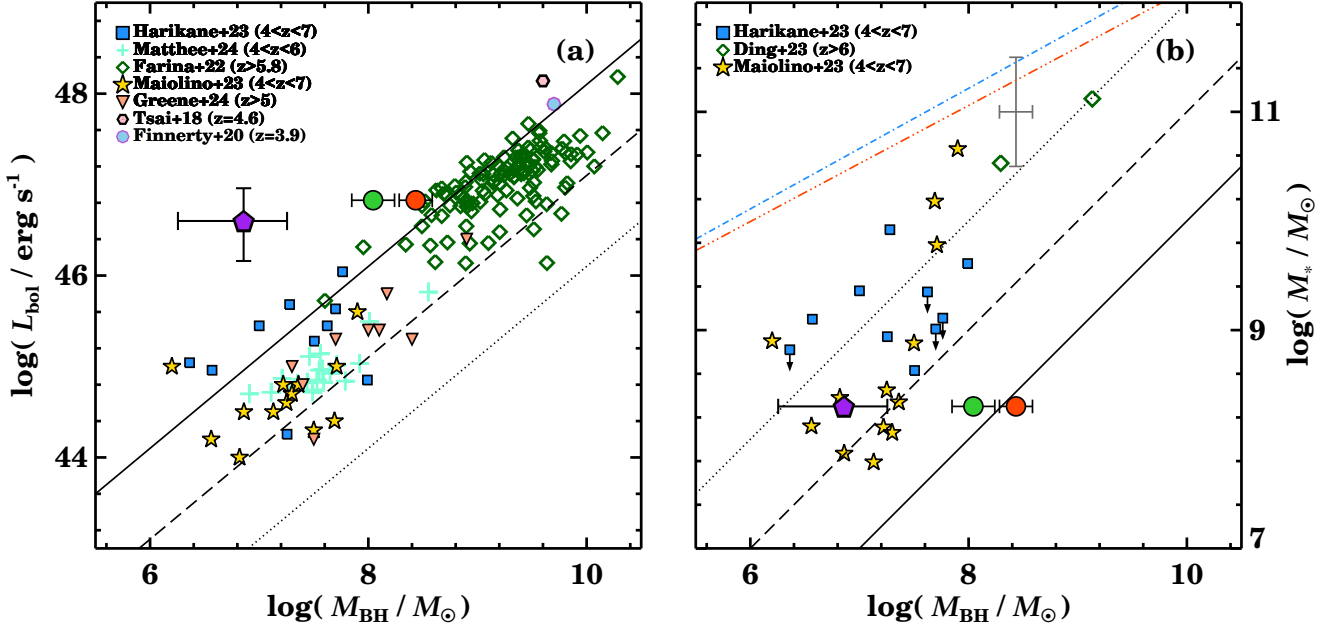


Figure 3. (a) M_{BH} vs. L_{bol} of LID-568 and quasars at similar redshifts. LID-568 is marked with circles, where the red and green circles represent the $L_{3.4}$ -based M_{BH} and the $L_{\text{H}\alpha}$ -based M_{BH} , respectively. The purple pentagon indicates the values measured in Suh et al. (2024). The solid, dashed, and dotted lines indicate λ_{Edd} of 1, 0.1, and 0.01, respectively. (b) Comparison of M_{BH} and M_{*} . The meanings of the red and green circles and purple pentagon are identical to those in panel (a). Gray error bar represents the $L_{3.4}$ -based M_{BH} and the M_{*} from the SFR of the host galaxy. The solid, dashed, and dotted lines mean M_{BH} -to- M_{*} ratio of 1, 0.1, and 0.01, respectively, and the dot-dashed blue and dot-dot-dot-dashed red lines represent disk-dominated and bulge-dominated AGNs in the nearby Universe (Zhuang & Ho 2023).

4.3. Host galaxy property

It is noteworthy that our M_{BH} value is comparable to the stellar mass (M_{*}) of the host galaxy (Suh et al. 2024). Suh et al. (2024) performed far-infrared (FIR) SED fitting extending to hundreds of microns, using a power-law and two greybody components (Casey 2012), and measured a total IR luminosity ($L_{8-1,000 \mu\text{m}}$) and dust mass of $\sim 2.95 \times 10^6 M_{\odot}$, respectively. Using the dust-to-stellar mass ratio at a similar redshift (Xiao et al. 2023), the M_{*} is found to be $\sim 2 \times 10^8 M_{\odot}$.

Alternatively, we estimated M_{*} based on star-formation rate (SFR) of the host galaxy. According to Suh et al. (2024), the observed specific flux at $870 \mu\text{m}$ of LID-568 is $545 \pm 158 \mu\text{Jy}$. Assuming that the rest-frame FIR flux is dominated by star formation, and approximating that the rest-frame wavelength of $175 \mu\text{m}$ of the sub-mm band to $160 \mu\text{m}$, we obtain SFR of $\sim 1000 M_{\odot} \text{ yr}^{-1}$ adopting the FIR-SFR correlation of Calzetti et al. (2010). From the observed SFR vs. M_{*} of starburst or luminous infrared galaxies (Rodighiero et al. 2011), we get $\log(M_{*}/M_{\odot}) = 10.5$ to 11.5.

Based on M_{*} from Suh et al. (2024), LID-568 has an M_{BH} -to- M_{*} ratio of ~ 1 , significantly higher than those

of other quasars at similar redshifts (Maiolino et al. 2023; Ding et al. 2023; Harikane et al. 2023) or AGNs in the nearby Universe (Zhuang & Ho 2023), as shown in Figure 3b. On the other hand, if we adopt our estimate of M_{*} , the M_{BH} to M_{*} ratio of LID-568 is comparable to that of other quasars at similar redshifts. More reliable measurements of M_{*} should resolve the differences in the M_{BH} to M_{*} ratios.

5. SUMMARY

We reanalyzed the JWST spectra of LID-568, an intriguing dust-obscured quasar at $z \sim 4$ whose SMBH has been suggested to be undergoing a super-Eddington accretion at $\lambda_{\text{Edd}} \sim 40$. However, our analysis that accounts for the heavy dust-extinction reveals that LID-568 seems undergoing Eddington-limited accretion at $\lambda_{\text{Edd}} \sim 1$. Our new M_{BH} value is about $10^{8.43} M_{\odot}$, ~ 40 times higher than that suggested by Suh et al. (2024), which is the reason for the discrepancy. These results emphasize the challenges and importance of dust-extinction correction in understanding the nature of dust-obscured quasars. Moreover, our IR-based analysis could better constrain the nature of newly discovered high- z dust-obscured quasars – often referred to as “little red dots” and found through JWST observations.

1 We thank Hyewon Suh for useful discussions, as well as
 2 the anonymous referee for constructive comments. This
 3 work is supported by the National Research Foundation
 4 of Korea (NRF) grant, No. 2020R1A2C3011091 and
 5 2021M3F7A1084525, funded by the Korea government
 6 (MSIT). D.K. acknowledges the support by the Na-
 7 tional Research Foundation of Korea (NRF) grant (No.
 8 2021R1C1C1013580 and 2022R1A4A3031306) funded
 9 by the Korean government (MSIT).

REFERENCES

- Assef, R. J., Kochanek, C. S., Brodwin, M., et al. 2010, *ApJ*, 713, 970
- Banerji, M., Alaghband-Zadeh, S., Hewett, P. C., et al. 2015, *MNRAS*, 447, 3368
- Calzetti, D., Wu, S.-Y., Hong, S., et al. 2010, *ApJ*, 714, 1256
- Casey, C. M. 2012, *MNRAS*, 425, 3094
- Civano, F., Marchesi, S., Comastri, A., et al. 2016, *ApJ*, 819, 62
- Decarli, R., Falomo, R., Treves, A., et al. 2010, *MNRAS*, 402, 2453
- Ding, X., Onoue, M., Silverman, J. D., et al. 2023, *Nature*, 621, 51
- Du, P. & Wang, J.-M. 2019, *ApJ*, 886, 42
- Du, P., Lu, K.-X., Zhang, Z.-X., et al. 2016, *ApJ*, 825, 126
- Farina, E. P., Schindler, J.-T., Walter, F., et al. 2022, *ApJ*, 941, 106
- Ferrarese, L., & Merritt, D. 2000, *ApJL*, 539, L9
- Finnerty, L., Larson, K., Soifer, B. T., et al. 2020, *ApJ*, 905, 16
- Fitzpatrick, E. L. 1999, *PASP*, 111, 63
- Gebhardt, K., Bender, R., Bower, G., et al. 2000, *ApJL*, 539, L13
- Georgakakis, A., Clements, D. L., Bendo, G., et al. 2009, *MNRAS*, 394, 533
- Glikman, E., Simmons, B., Maily, M., et al. 2015, *ApJ*, 806, 218
- Gordon, K. D., Clayton, G. C., Misselt, K. A., et al. 2003, *ApJ*, 594, 279
- GRAVITY Collaboration, Amorim, A., Bourdarot, G., et al. 2024, *A&A*, 684, A167
- Greene, J. E. & Ho, L. C. 2005, *ApJ*, 630, 122
- Greene, J. E., Labbe, I., Goulding, A. D., et al. 2024, *ApJ*, 964, 39
- Harikane, Y., Zhang, Y., Nakajima, K., et al. 2023, *ApJ*, 959, 39
- Hopkins, P. F., Hernquist, L., Cox, T. J., et al. 2006, *ApJS*, 163, 1
- Hopkins, P. F., Hernquist, L., Cox, T. J., & Kereš, D. 2008, *ApJS*, 175, 356
- Im, M., Griffiths, R. E., & Ratnatunga, K. U. 1997, *ApJ*, 475, 457
- Jun, H. D., Assef, R. J., Bauer, F. E., et al. 2020, *ApJ*, 888, 110
- Kim, D., Im, M., & Kim, M. 2010, *ApJ*, 724, 386
- Kim, D., Im, M., Glikman, E., et al. 2015, *ApJ*, 812, 66
- Kim, D. & Im, M. 2018, *A&A*, 610, A31
- Kim, D., Im, M., Canalizo, G., et al. 2018, *ApJS*, 238, 37
- Kim, D., Im, M., Kim, M., et al. 2020, *ApJ*, 894, 126
- Kim, D., Lee, D., & Im, M. 2022, *MNRAS*, 509, 1147
- Kim, D., Im, M., Kim, M., et al. 2023, *ApJ*, 954, 156
- Kim, D., Im, M., Lim, G., et al. 2024, *Journal of Korean Astronomical Society*, 57, 95
- Kim, D., Kim, Y., Im, M., et al. 2024, *A&A*, 690, A283
- Kormendy, J., & Ho, L. C. 2013, *ARA&A*, 51, 511
- Krawczyk, C. M., Richards, G. T., Mehta, S. S., et al. 2013, *ApJS*, 206, 4
- Lynden-Bell, D. 1969, *Nature*, 223, 690
- Madau, P., Pozzetti, L., & Dickinson, M. 1998, *ApJ*, 498, 106
- Maiolino, R., Scholtz, J., Curtis-Lake, E., et al. 2023, *arXiv:2308.01230*
- Marchesi, S., Civano, F., Elvis, M., et al. 2016, *ApJ*, 817, 34
- Markwardt, C. B. 2009, *Astronomical Data Analysis Software and Systems XVIII*, 411, 251
- Matthee, J., Naidu, R. P., Brammer, G., et al. 2024, *ApJ*, 963, 129
- Planck Collaboration, Ade, P. A. R., Aghanim, N., et al. 2016, *A&A*, 594, A13
- Polletta, M., Weedman, D., Hönig, S., et al. 2008, *ApJ*, 675, 960-984
- Richards, G. T., Lacy, M., Storrie-Lombardi, L. J., et al. 2006, *ApJS*, 166, 470

- Rodighiero, G., Daddi, E., Baronchelli, I., et al. 2011, ApJL, 739, L40
- Shen, Y., Greene, J. E., Ho, L. C., et al. 2015, ApJ, 805, 96
- Suh, H., Civano, F., Trakhtenbrot, B., et al. 2020, ApJ, 889, 32
- Suh, H., Scharwächter, J., Farina, E. P., et al. 2024, Nature Astronomy
- Tsai, C.-W., Eisenhardt, P. R. M., Jun, H. D., et al. 2018, ApJ, 868, 15
- Urrutia, T., Lacy, M., & Becker, R. H. 2008, ApJ, 674, 80-96
- Urrutia, T., Lacy, M., Spoon, H., et al. 2012, ApJ, 757, 125
- Woo, J.-H., Treu, T., Malkan, M. A., et al. 2008, ApJ, 681, 925
- Xiao, M.-Y., Elbaz, D., Gómez-Guijarro, C., et al. 2023, A&A, 672, A18
- Zhuang, M.-Y. & Ho, L. C. 2023, Nature Astronomy, 7, 1376